Additive Manufacturing: Metallurgy, Cut Analysis & Porosity

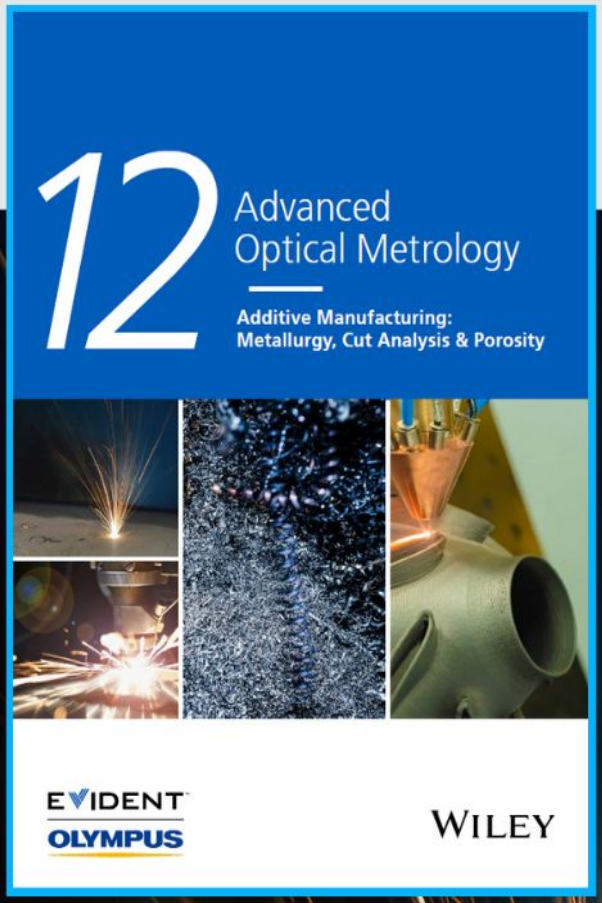

The latest eBook from Advanced Optical Metrology. Download for free.

In industry, sector after sector is moving away from conventional production methods to additive manufacturing, a technology that has been recommended for substantial research investment.

Download the latest eBook to read about the applications, trends, opportunities, and challenges around this process, and how it has been adapted to different industrial sectors.

EVIDENT
OLYMPUS

WILEY

IET Electric Power Applications

Research Article

IET Journals
The Institution of Engineering and Technology

New elevator system constructed by multi-translator linear switched reluctance motor with enhanced motion quality

ISSN 1751-8660
Received on 7th December 2019
Revised 26th April 2020
Accepted on 12th May 2020
E-First on 1st July 2020
doi: 10.1049/iet-epa.2019.0996
www.ietdl.org

Siamak Masoudi[1] ✉, *Hasan Mehrjerdi*[2], *Amir Ghorbani*[1]

[1]*Department of Electrical Engineering, Islamic Azad University, Abhar Branch, Abhar, Iran*
[2]*Department of Electrical Engineering, Qatar University, Doha, Qatar*
✉ *E-mail: s.masoudi@tabrizu.ac.ir*

Abstract: In this work, a new elevator system created by a linear switched reluctance motor is presented. Unlike conventional linear motors, the proposed linear motor has more than one translator. Each phase in a translator generates a pulsing force; hence, the total generated force has noticeable ripple making it difficult to soft motion. In order to solve this problem, similar phases in different translators have been located in positions with specified distances together. As a result, similar force pulses would be shifted so that they can compensate together. An appropriate control strategy has been designed for the system, which can control the current, force, speed, and position simultaneously. A conventional proportional–integral controller and an adaptive fuzzy controller have been used to control the speed. In order to have a precise study, a prototype elevator system along with its control unit has been made and the obtained results have been compared with the simulation results. These results confirm that the proposed structure can significantly produce force and speed ripples.

1 Introduction

Switched reluctance motors (SRMs) are attractive electrical machines and have advantages such as low cost, high reliability, and robustness. They have a very simple structure with only one set of winding on stator while their rotor has no winding or permanent magnet. The development of power electronic converters and their control strategies cause SRMs to be used in various applications that they could not be used in the past. In some industrial applications including direct movement, the linear-type motors can be very useful for eliminating the mechanical converters. Linear SRMs (LSRMs) have different structures [1]. In a single-side LSRM, in addition to propulsion force there is a force in the vertical direction of motion, while double-sided LSRMs can produce more propulsion force with about zero vertical force. The main disadvantage of SRMs (or LSRMs) is their high torque (or force) ripple which may limit their applications. In recent decades many studies have been done to solve the problem either by motor design [2–4] or control methods [5–13]. It has been proven in some articles that using an appropriate force distribution function (FDF) in the LSRM control system can be very useful in force ripple minimisation [5–7]. An instantaneous torque control strategy in an SRM has been presented in [8]. Another modified torque control approach based on finite-state prediction in an SRM has been illustrated in [9]. It has been shown that the approach can minimise the copper loss, switching frequency, and the torque ripple simultaneously although it requires a precise mathematical model of the motor. An interesting method has been suggested in [10] that a new power electronic converter has led to a significant reduction in the rise and fall times of phase current and finally decreases the torque ripple. Moreover, there are other control strategies presented by researchers that may be effective in force (or torque) ripple minimisation. Many articles have investigated the application of fuzzy logic-based approaches in SRM control [11]. The fuzzy logic can be used along with other methods such as the adaptive control method or sliding mode control method. In [12], the fuzzy logic has been used to model the non-linear structure of an LSRM in an adaptive control strategy. It has been illustrated that the model has high robustness in parameter uncertainty and motor non-linear behaviour. In another article, type 2 Takagi–Sugeno fuzzy system has been used to approximate an LSRM [13]. In order to overcome the uncertainty problem, upper and lower membership functions have been considered for fuzzy modelling used in an adaptive sliding mode control method.

LSRMs have been used as an actuator in ropeless elevators in some previous works [3, 7, 14, 15]. The systems have shown some important advantages such as low required area, eliminating the mechanical converters, and precise speed and position control. Different structures of LSRMs may be used in elevator application but the LSRM designed in [14, 15] has a high force to mass density, therefore is an appropriate choice for vertical motion. The optimal design of an LSRM used in the elevator application has been presented in [3]. In order to improve the motion quality and reduce the force ripple, a new FDF along with a jerk minimisation strategy has been proposed in [7]. To enhance the efficiency of the elevator system, a perfect control system has been presented in [14, 15] which could control the position, speed, current, and force simultaneously.

In this work we use an LSRM with only one double-sided stator while more than one active translator is located between two stator sides [7]. Translators are positioned in the specified distance together so that the force drop of each translator can be compensated by the other translators peak force. Optimised distance is obtained based on both force ripple minimisation and average force maximisation. An appropriate control system is designed which is able to control the current and force of different translators.

2 Prototype system description

2.1 Elevator structure

A multi-translator LSRM (MLSRM) is used in this work to make an elevator system. The motor has four phases on each translator which two phases are ON and two other phases are OFF at any time. Schematic of the proposed linear motor consisting of two translators and the elevator system consisting of two MLSRMs are shown in Fig. 1. According to the figure the force required to move the cabin is prepared by four translators.

2.2 MLSRM modelling

SRMs are non-linear systems that their inductance and force depend on current and position. In order to have a precise analysis of these motors it is necessary to have an accurate model of

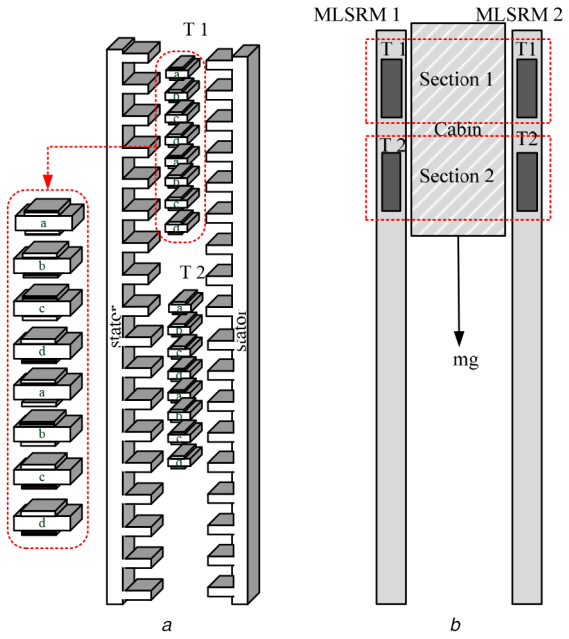

Fig. 1 *Elevator system and MLSRM*
(a) An MLSRM, ***(b)*** Elevator system with two MLSRM

inductance. In this work, we use the inductance model approach presented in [5] which introduced the phase inductance using three equations such as

$$L(i,x)=\begin{cases}\left(Ax^2+Bx+C_1\right).k(i,x)\\ \left(Dx+C_2\right).k(i,x)\\ \left(Ex^2+Fx+C_1\right).k(i,x)\end{cases} \tag{1}$$

where $k(i,x)=ax^3+bx^2+cx+d$. After finite element analysis of the MLSRM and using the curve fitting method, all parameters of the inductance are obtained for different currents. The propulsion force of a phase can be obtained using the following equation:

$$F=\frac{1}{2}i^2\frac{\partial L(i,x)}{\partial x} \tag{2}$$

2.3 Modelling of the elevator system

Assuming that F_k^* and F_t^* are the reference force of kth translator and the total required force, respectively, we can write

$$F_t^*=\sum_{k=1}^{N}F_k^* \tag{3}$$

where N is the total number of translators. Considering that two phases of a translator are ON at any time then

$$F_k^*=F_{km}^*+F_{kn}^*=\frac{1}{2}\left(i_{km}^2+i_{kn}^2\right)\frac{\partial L_k}{\partial x} \tag{4}$$

where m and n may be one of the phases a, b, c, or d.

3 Proposed structure

3.1 Purpose description

In a conventional structure, translators of an MLSRM are located in the same situations so that their peak forces occur in the same time and position. This causes the total produced force to have a high peak value, but it seems that ripple also gets stronger. To solve this problem, we propose that translators of an MLSRM are located in specified positions where their peak force occurs in different positions; therefore, the drop can be compensated and ripple may be reduced. This is shown in Fig. 2, in which translator 2 (T2) is located so that its produced peak force happens in distance α from the peak force of T1.

According to Fig. 1, and assuming that two MLSRM with N translators are used, total force applied to the cabin can be calculated as

$$\begin{aligned}F_t(i_{km},i_{kn},x)=&\frac{1}{2}\left(i_{1m}^2+i_{1n}^2\right)\frac{\partial L_1(x)}{\partial x}+\frac{1}{2}\left(i_{2m}^2+i_{2n}^2\right)\frac{\partial L_2(x)}{\partial x}\\&+\cdots+\frac{1}{2}\left(i_{Nm}^2+i_{Nn}^2\right)\frac{\partial L_N(x)}{\partial x}\end{aligned} \tag{5}$$

where α_k denotes the movement of the kth translator with respect to the master translator (T1). Electromagnetic characteristics of all translators are the same with only a specified displacement equal to α, so we can write $L_2(x)=L_1(x+\alpha_1),\ldots,L_N(x)=L_1(x+\alpha_N)$.

In order to have a precise study of the proposed system, some parameters are required such as average force over a cycle (F_{av}), the effective force (F_{rms}), ac component of the force (F_{ac}), and ripple factor (RF). These parameters are introduced as follows:

$$F_{\mathrm{av}}=\frac{1}{T_{\mathrm{sp}}}\int_0^{T_{\mathrm{sp}}}F_t(i_{km},i_{kn},x)\mathrm{d}x \tag{6}$$

$$F_{\mathrm{rms}}=\sqrt{\frac{1}{T_{\mathrm{sp}}}\int_0^{T_{\mathrm{sp}}}F_t^2(i_{km},i_{kn},x)\mathrm{d}x} \tag{7}$$

$$F_{\mathrm{ac}}=\sqrt{F_{\mathrm{rms}}^2-F_{\mathrm{av}}^2} \tag{8}$$

$$\mathrm{RF}=\frac{F_{\mathrm{ac}}}{F_{\mathrm{av}}} \tag{9}$$

3.2 Optimisation of parameter α

In this section calculation of the optimised α is presented. For this purpose, objective functions including the force ripple and average force are introduced as follows:

$$f_{0\_1}(\underline{z})=\frac{1}{F_{\mathrm{av}}} \tag{10}$$

$$f_{0\_2}(\underline{z})=\mathrm{RF} \tag{11}$$

where z denotes a set of variables which can be set to minimise the functions $f_{0\_1}(\underline{z})$ and $f_{0\_2}(\underline{z})$. In this work, $\underline{z} = (\alpha)$. We used a multi-objective seeker optimisation algorithm for the optimisation problem. The multi-objective optimisation function can be written as

$$f = \min\{f_{0\_1},\ f_{0\_2}\} \tag{12}$$

The optimisation algorithm has been described in [4] completely. Optimisation results for systems consisting of two and three translators in each MLSRM are demonstrated in Fig. 3. It can be seen that in a two translator motor, f is minimum if the second translator shifted as 6.5 mm with respect to the first translator. In addition, in a three-section motor, the objective function f is minimum when translators 2 and 3 are shifted positionally about 4.2 and 8.4 mm, respectively.

4 Control system

The importance of position and speed control in an elevator is obvious. The existence of a smooth raise force can guarantee the motion quality of the cabin in the elevator. For this, an appropriate total force should be generated in any position. The amount of the required total force is calculated according to the weight of the moving part, speed, and desired acceleration. This force should be prepared by all translators; therefore, the contribution of each translator can be determined. This force is divided between four phases of the translator by an appropriate FDF [7]. Fig. 4 indicates the force and current control units in the proposed drive system. The block diagram of the proposed control system including four controllers i.e. cascade current, force, speed, and position is shown in Fig. 5. Reference speed generator may be a trapezoidal profile, which is based on the desired speed and the difference between the final desired position and actual position. In this work we use a jerk minimisation-based speed profile which is effective in the elevator cabin jerk minimisation. A conventional proportional–integral (PI) controller has been used to regulate the motor current while the speed control has been done by two methods: a conventional PI controller and a new adaptive fuzzy control discussed in our previous work [12]. PI controllers have been designed based on the error-trial method while the proportional and integral gains of the PI speed controller have been obtained as 1.2 and 0.8, respectively. Similarly, the proportional and integral gains of the PI current controller have been extracted as 5.3 and 2.5, respectively. Also, the required parameters for the adaptive fuzzy controller [12] have been obtained as $\lambda = 10$, $\delta = 1$, $\Gamma_1 = 35$, $\Gamma_2 = 18$, $\alpha_1 = 0.005$, $\alpha_2 = 0.002$. These parameters were obtained for a system consisting of two MLSRMs with two translators.

The control system is common for all motors, while two distinct half bridge converters have been used for two sections indicated in Fig. 1. This increases the reliability of the system. ON and OFF

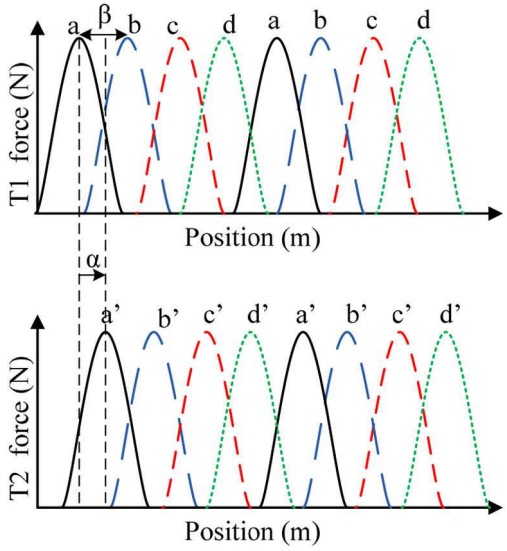

Fig. 2 *Forces produced by two translators of an MLSRM*

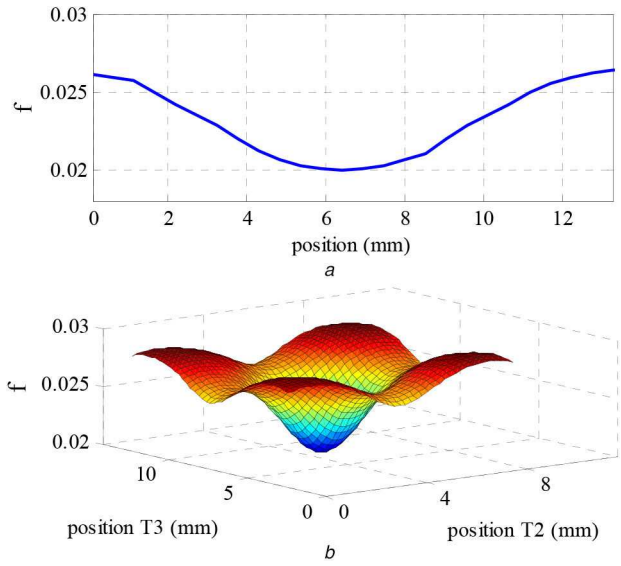

Fig. 3 *Optimised position of translator*
(a) Two translator MLSRM, ***(b)*** Three translator MLSRM

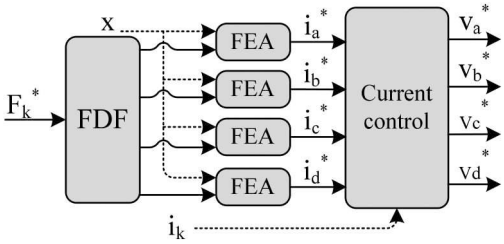

Fig. 4 *FDF and current controller*

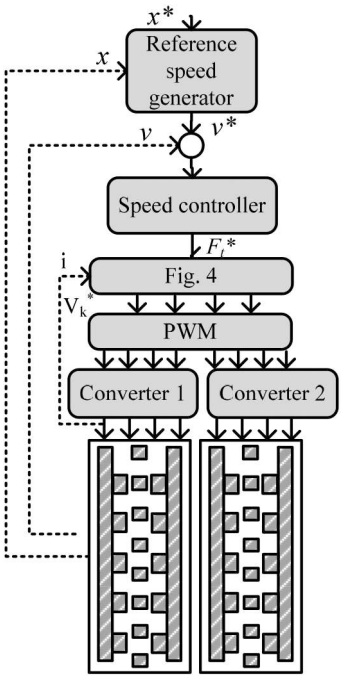

Fig. 5 *Proposed control system*

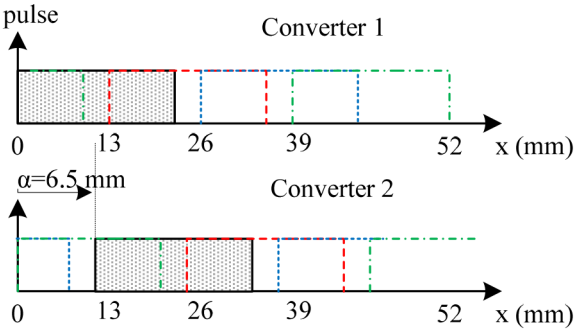

Fig. 6 *PWM pulses for two converters*

positions are different for switches of two converters, but according to the previous section there is a certain shift between them. Consequently, after calculating the firing position of switches in the first converter, it may be easily obtained for the second converter. Firing pulses of the first and second converters are shown in Fig. 6. It can be seen that any switch of converter 2 becomes ON or OFF after 6.5 mm with respect to the similar switch in converter 1.

5 Simulation results

The proposed elevator system consists of two MLSRMs on both sides of the cabin. Each MLSRM has two translators between a double-sided stator; consequently, four translators generate the force required to move the cabin. Parameters and dimensions of the proposed LSRM are written in Table 1. These parameters are obtained and optimised in our previous work [4].

The control system indicated in Fig. 5 was applied to the proposed system and the performance of the system was studied. Results are shown for four below states:

- conventional construction, conventional PI controller;
- proposed construction, conventional PI controller;
- conventional construction, adaptive fuzzy controller;
- proposed construction, adaptive fuzzy controller.

Simulation results for the cabin movement at speed 0.5 m/s and from 0 to height 1 m are shown in Fig. 7. The first curve demonstrates the position and speed of the cabin. It can be seen that the cabin reaches a height of 1 m in about $t = 2.1$ s. In the period, the motor is accelerated to reach the speed 0.5 m/s and then moves at a constant speed to get to the point where it has to stop. After this point, the speed slows down for about 0.1 s to stop the cabin. A similar process occurs when the engine goes down. The total force generated by four translators is shown in Fig. 7*b*. It is

Table 1 Parameters of the proposed LSRM

Variable	Value, mm
air gap length, mm	2
stator pole width, mm	24.1
stator slot width, mm	31
stator pole height, mm	25.2
translator pole width, mm	12.3
translator pole height, mm	45.4
translator height, mm	220
winding turns	200
rated current, A	10
rated voltage, V	150
coefficient of friction, *C*	10 N/m/s
weight of translator, *M*	7 kg
total weight of cabin	30 kg
phase resistance	2.5 Ω

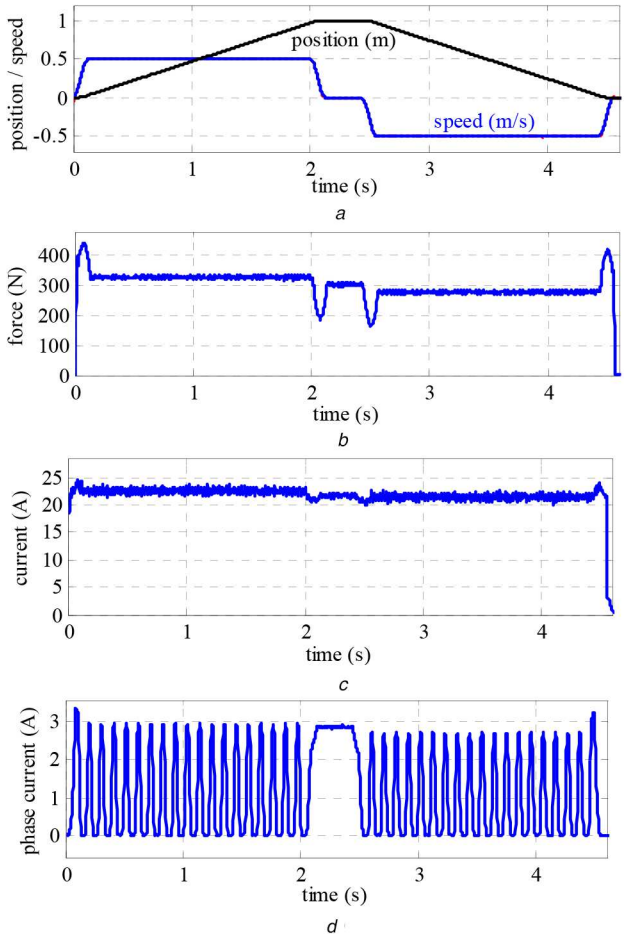

Fig. 7 *Simulation results at speed 0.5 m/s*
(a) Position and speed, ***(b)*** Total force, ***(c)*** Current of source, ***(d)*** Phase current

obvious that the force is higher at acceleration periods while it is lower at deceleration times. However, a positive force is continually required to protect the cabin from falling. Also, due to gravity, the amount of force at the time of ascent is greater than at the time of descent. This can be seen in the current curves in Figs. 7*c* and *d*.

According to Fig. 8, at each time, two phases are ON and are contributing to the force generation. Comparison shows that the peak force of the same phases in two translators occurs at different points. This can prevent a sharp drop in total force and thus reduces the ripple in force and speed. In order to show the efficiency of the proposed structure, force and speed curves for different mentioned constructions are illustrated in Figs. 9 and 10, respectively. It can be seen that the proposed structure can reduce the force and speed ripple significantly, while the ripple is lowest when the proposed construction is controlled by the adaptive fuzzy controller.

For further study, the performance of the system was investigated at different speeds and cabin weights. Results obtained from these studies are shown in Fig. 11. The per cent of ripple factor at different points has been calculated by (9). According to Fig. 11, the conventional structure with a usual PI speed controller has the highest per cent of ripple, while with increasing speed and cabin weight, the ripple increases. Using the new MLSRM structure or using the new speed controller, the amount of fluctuation is significantly reduced. This can be seen in curves 2 and 3 of Fig. 11. Finally, combining the new MLSRM structure with the new speed controller leads to minimal fluctuations in force and speed.

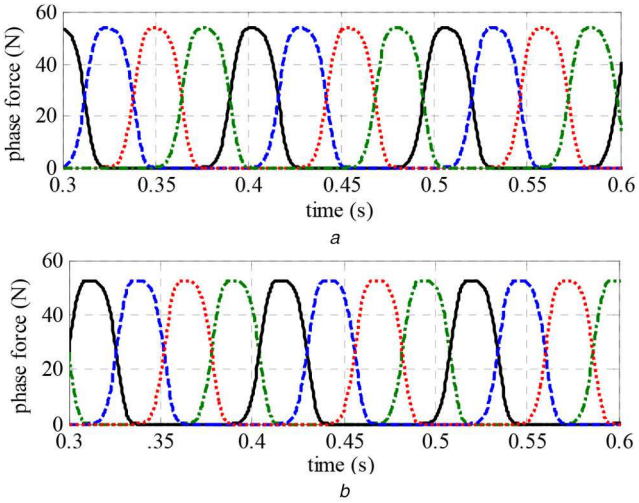

Fig. 8 *Phase force comparison*
(a) Translator 1, ***(b)*** Translator 2 (displaced translator)

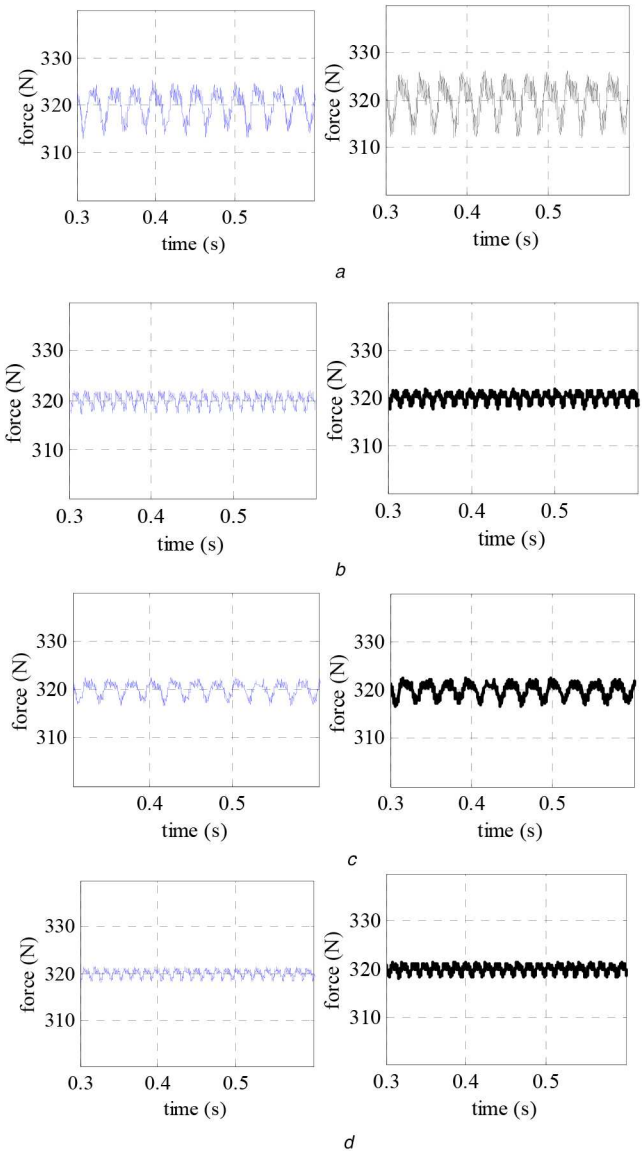

Fig. 9 *Force ripple comparison*
(a) Conventional construction and controller, ***(b)*** Proposed construction, conventional controller, ***(c)*** Conventional construction, adaptive fuzzy controller, ***(d)*** Proposed construction, adaptive fuzzy controller

6 Experimental results

The strategy was applied to the prototype elevator system. The performance of the system at speed 0.5 m/s with 32 kg weight of the cabin was studied and the obtained results are shown in Fig. 12. After storing the signals in flash memory, they were plotted by a curve fitting toolbox in Matlab/Simulink software. The total force

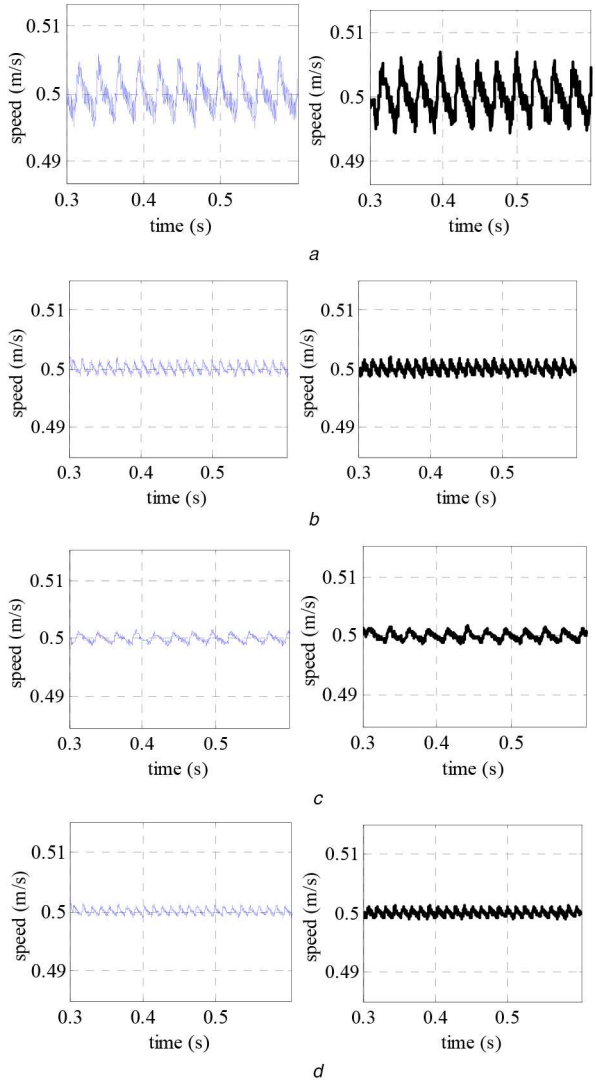

Fig. 10 *Speed ripple comparison*
(a) Conventional construction and controller, ***(b)*** Proposed construction, conventional controller, ***(c)*** Conventional construction, adaptive fuzzy controller, ***(d)*** Proposed construction, adaptive fuzzy controller

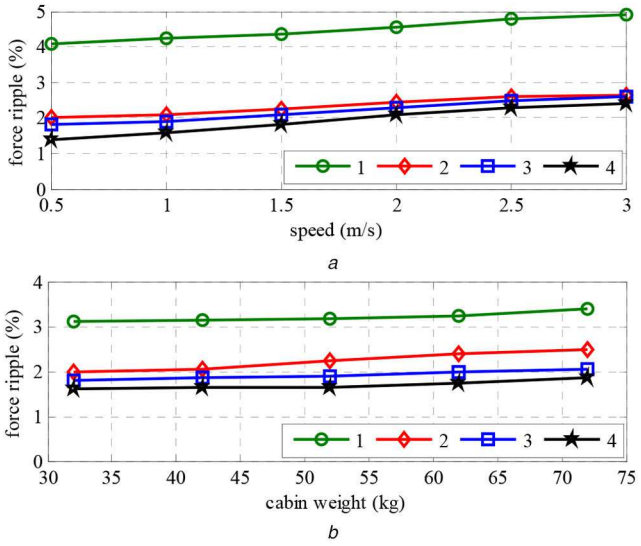

Fig. 11 *Force and speed ripple comparison*
(a) Different speeds, ***(b)*** Different cabin weights
1: conventional construction and controller; 2: proposed construction, conventional controller; 3: conventional construction, adaptive fuzzy controller; 4: proposed construction, adaptive fuzzy controller

generated by four translators and force of each translator were calculated based on the measured parameters and related equations. These are shown in Fig. 13. A comparison of total propulsion force and speed ripples for four different constructions is shown in Figs. 9 and 10.

Currents measured in the above test are illustrated in Fig. 14. The current of the source, which is the sum of the whole four translators, is shown in Fig. 14*a*. The phase current of each translator is shown in Fig. 14*b*.

As mentioned, the second translator in the proposed elevator system has a shift from the first translator positionally, so at a certain point, the amount of force produced in the same phases of two translators is different. Thus, the amount of current in the same phases of the two translators is also different. A few cycles of current waveforms of phase A in two translators (main and displaced one) are indicated in Fig. 15.

In order to have a precise comparison of results between different constructions and controllers, force and speed ripples measured by simulation and experimental are indicated in Table 2. According to the results, the proposed structure has significantly better performance than the conventional structure both in simulation and experiment. Similar to the previous results, the proposed construction along with the new adaptive fuzzy controller has the best performance over the others.

In the prototype system we have used MLSRMs with two translators in a common double-sided stator. Each LSRM has been designed for a maximum speed of 3 m/s and maximum load equal to 10 kg (apart from the weight of the book itself, which is 8 kg). In

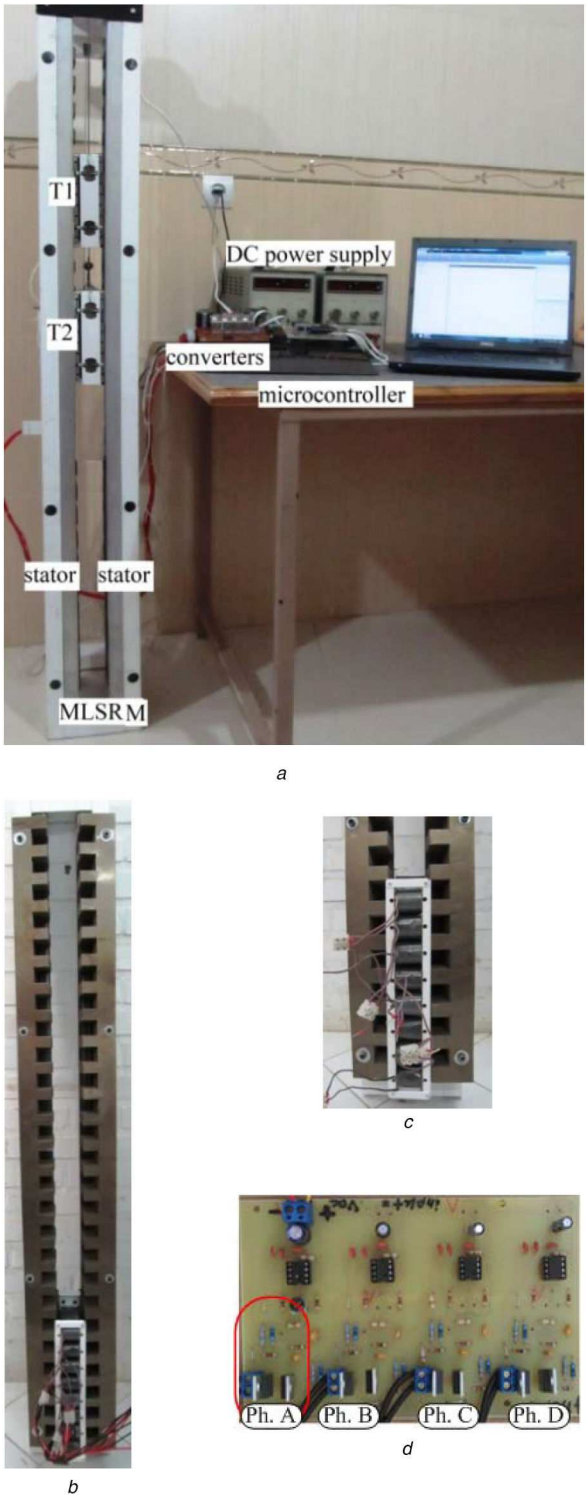

Fig. 12 *Experimental setup*
(a) Laboratory setup, ***(b)*** One stator with one translator, ***(c)*** Translator, ***(d)*** Half -bridge four-phase converter

order to have a precise study on the performance of the system, we have tested experimentally each MLSRM with only one translator at different speeds and loads. Fig. 16 indicates the experimental measurement force from speeds of 0.5 m/s to more than the maximum speed of 3 m/s. At speeds of <3 m/s, the speed is almost constant, after which the LSRM enters the constant power or field weakening region.

7 Conclusion

In this work, a new structure of an elevator system using LSRMs was presented. Each linear motor has several translators located in the optimised distance together. Optimisation was done based on the minimisation of total force ripple. An appropriate control strategy was designed and applied to the system which consists of four control units: current controller, force controller, speed controller, and position control unit. The current controller is a conventional PI one while two PI and adaptive fuzzy speed controllers are used to investigate the system performance. In order to convince the performance of the proposed system, a prototype system was constructed and studied along with the simulation results. The obtained results confirmed the good efficiency of the system.

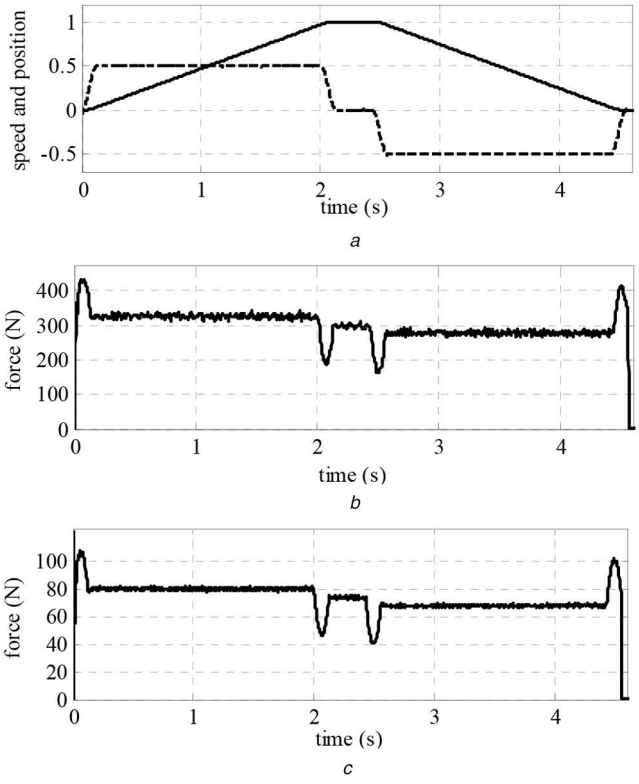

Fig. 13 *Experimental results*
(a) Speed and position, ***(b)*** Total force, ***(c)*** Translator force

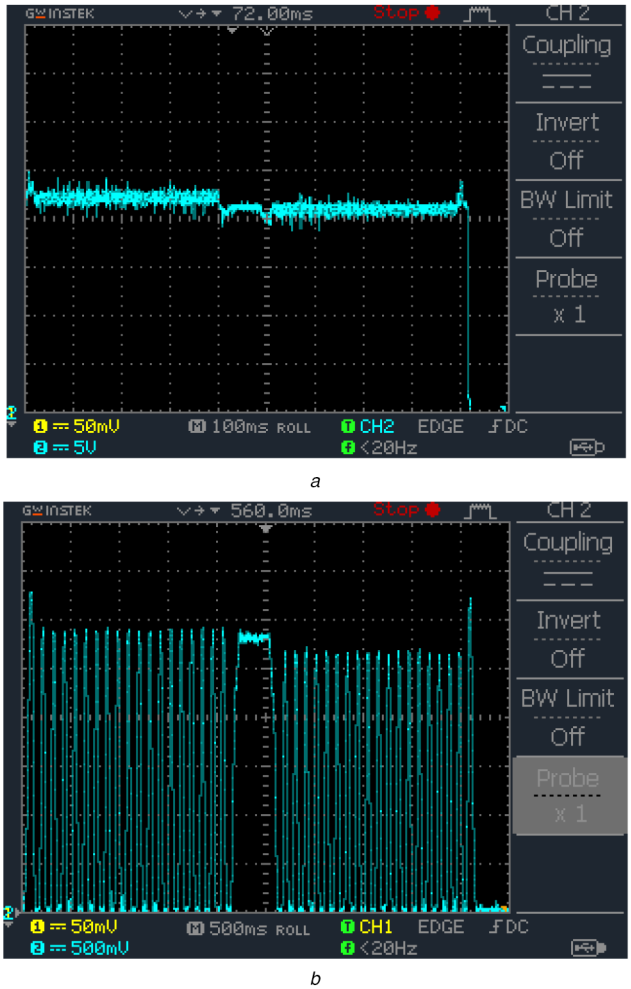

Fig. 14 *Measured currents*
(a) Current of source, ***(b)*** Each translator

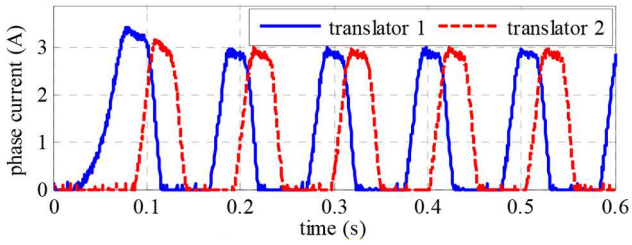

Fig. 15 *Phase current comparison*

Table 2 Force and speed ripple with weight variations

Weight		Force ripple, %			Speed ripple, %				
	1	2	3	4	1	2	3	4	
32	sim	3.1	2	1.85	1.65	16	6	4	3
	exp	3.1	2	1.9	1.65	16	7	5	3
42	sim	3.15	2.05	1.9	1.6	16.5	7	4	3
	exp	3.2	2.1	2	1.65	17	7	5	3.5
52	sim	3.2	2.3	1.95	1.7	16.5	6.5	4.5	3.5
	exp	3.2	2.35	2	1.7	17	7	5	4
62	sim	3.3	2.4	2	1.8	18	6.5	5	4
	exp	3.3	2.5	2.05	1.9	18	7.5	5	4.5
72	sim	3.4	2.55	2.05	1.9	18	8	6	4.5
	exp	3.45	2.65	2.1	2	19	9	6.5	5

1: Conventional construction and controller; 2: proposed construction, conventional controller; 3: conventional construction, adaptive fuzzy controller; 4: proposed construction, adaptive fuzzy controller.

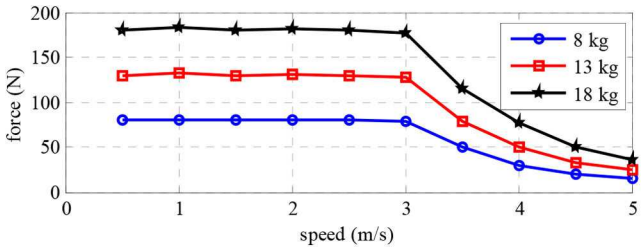

Fig. 16 *Experimental results at different speeds and loads*

8 References

[1] Lobo, N.S., Lim, H.S., Krishnan, R.: 'Comparison of linear switched reluctance machines for vertical propulsion application: analysis, design and experimental correlation', *IEEE Trans. Ind. Appl.*, 2008, **44**, (4), pp. 1134–1142

[2] Sheikhi, A., Oraee, H., Kaboli, S., *et al.*: 'A new configuration of switched reluctance motor for reducing the torque ripple'. Int. Conf. on Electric Power and Energy Conversion Systems, Sharjah, UAE, 2009

[3] Wang, D., Du, X., Zhang, D., *et al.*: 'Design, optimization, and prototyping of segmental-type linear switched reluctance motor with a toroidally wound mover for vertical propulsion application', *IEEE Trans. Ind. Electron.*, 2017, **65**, (2), pp. 1865–1874

[4] Soltanpour, M., Abdollahi, H., Masoudi, S.: 'Optimisation of double-sided linear switched reluctance motor for mass and force ripple minimisation', *IET Sci. Meas. Technol.*, 2019, **13**, (4), pp. 509–517

[5] Pan, J.F., Cheung, N.C., Zou, Y.: 'An improved force distribution function for linear switched reluctance motor on force ripple minimization with nonlinear inductance modelling', *IEEE Trans. Magn.*, 2012, **48**, (11), pp. 3064–3067

[6] Xue, X.D., Cheng, K.W.E., Ho, S.L.: 'Optimization and evaluation of torque-sharing functions for torque ripple minimization in switched reluctance motor drives', *IEEE Trans. Power Electron.*, 2009, **24**, (9), pp. 2076–2090

[7] Masoudi, S., Feyzi, M.R., Sharifian, M.B.B.: 'Force ripple and jerk minimization in double sided linear switched reluctance motor used in elevator application', *IET Electr. Power Appl.*, 2016, **10**, (6), pp. 508–516

[8] Moron, C., Garcia, A., Tremps, E., *et al.*: 'Torque control of switched reluctance motors', *IEEE Trans. Magn.*, 2012, **48**, (4), pp. 1661–1664

[9] Li, C., Wang, G., Li, Y., *et al.*: 'An improved finite-state predictive torque control for switched reluctance motor drive', *IET Electr. Power Appl.*, 2018, **12**, (1), pp. 144–151

[10] Muthulakshmi, P.S., Dhanasekaran, R.: 'A new modified switched reluctance motor drive using passive network for torque ripple minimisation'. Int. Conf. on Communications and Signal Processing, Melmaruvathur, India, 2015

[11] Li, H., Pan, Y., Shi, P., *et al.*: 'Switched fuzzy output feedback control and its application to mass-spring-damping system', *IEEE Trans. Fuzzy Syst.*, 2016, **24**, (6), pp. 1259–1269

[12] Masoudi, S., Soltanpour, M., Abdollahi, H.: ' a ew control method for a linear switched reluctance motor', *IET Electr. Power Appl.*, 2018, **12**, (9), pp. 1328–1336

[13] Azadrou, A., Masoudi, S., Ghanizadeh, R., *et al.*: 'New adaptive fuzzy sliding mode scheme for speed control of linear switched reluctance motor', *IET Electr. Power Appl.*, 2019, **13**, (8), pp. 1141–1149

[14] Lim, H.S., Krishnan, R.: 'Ropeless elevator with linear switched reluctance motor drive actuation systems', *IEEE Trans. Ind. Electron.*, 2007, **54**, (4), pp. 2209–2217

[15] Lim, H.S., Krishnan, R., Lobo, N.S.: 'Design and control of a linear propulsion system for an elevator using linear switched reluctance motor drives', *IEEE Trans. Ind. Electron.*, 2008, **55**, (2), pp. 534–542